Robust Signatures of Quantum Radiation Reaction in Focused Ultrashort Laser Pulses

Jian-Xing Li,* Karen Z. Hatsagortsyan,† and Christoph H. Keitel‡
Max-Planck-Institut für Kernphysik, Saupfercheckweg 1, 69029 Heidelberg, Germany
(Received 15 May 2014; published 23 July 2014)

Radiation-reaction effects in the interaction of an electron bunch with a superstrong focused ultrashort laser pulse are investigated in the quantum radiation-dominated regime. The angle-resolved Compton scattering spectra are calculated in laser pulses of variable duration using a semiclassical description for the radiation-dominated dynamics and a full quantum treatment for the emitted radiation. In dependence of the laser-pulse duration we find signatures of quantum radiation reaction in the radiation spectra, which are characteristic for the focused laser beam and visible in the qualitative behavior of both the angular spread and the spectral bandwidth of the radiation spectra. The signatures are robust with respect to the variation of the electron and laser-beam parameters in a large range. Qualitatively, they differ fully from those in the classical radiation-reaction regime and are measurable with presently available laser technology.

DOI: 10.1103/PhysRevLett.113.044801 PACS numbers: 41.60.-m, 12.20.Ds, 41.75.Ht, 42.65.Ky

Recent advances in strong-field laser techniques have enabled the development of novel all-optical x- or γ-ray radiation sources [1–3], which are beneficial for broad applications, see, e.g., [4,5]. In particular, x or γ rays are achieved via Compton backscattering of laser radiation off a relativistic electron beam [6,7]. In superstrong laser fields the Compton scattering acquires nonlinear characteristics due to multiple laser photon absorption [8–11]. Moreover, in strong fields, multiple photon emission during a laser period can be very likely. Consequently, the electron dynamics can be modified due to radiation, causing radiation-reaction (RR) effects [3,12]. Although the RR problem has been discussed since the early days of classical [13–16] and quantum [17–20] electrodynamics, the theory has not yet been tested experimentally. The development of the extreme light infrastructure [5] opens new perspectives to observe RR effects in laser-matter interaction at extreme conditions, and it has revived the interest in this problem [3,21–39].

The quantum effects in multiphoton Compton scattering (the photon recoil and spin effects) are governed by the invariant parameter $\chi \equiv |e|\sqrt{(F_{\mu\nu}p^\nu)^2}/m^3$ [11,40], where $F_{\mu\nu}$ is the field tensor, $p^\nu = (\varepsilon, \mathbf{p})$ the incoming electron four-momentum, and e and m are the electron charge and mass, respectively (Planck units $\hbar = c = 1$ are used throughout). In particular, the recoil of the emitted photon can be estimated as $\chi \sim \omega/\varepsilon$, with the emitted photon energy ω [3] and the quantum regime of radiation setting in at $\chi \gtrsim 1$. Physically, the parameter χ equals the ratio $\chi = E'/E_S$ of the laser field E' in the electron rest frame over the critical Schwinger field $E_S = m^2/|e|$ [41]. The laser intensity corresponding to the Schwinger field is $I_S = E_S^2/(8\pi) \approx 2.3 \times 10^{29}$ W/cm^2 which cannot be reached with realistic lasers [5,42]. However, a relativistic electron counterpropagating with the laser field may experience the Schwinger field in its rest frame $E' \approx 2\gamma E$, i.e., due to the Lorentz boost of the laser field E with the Lorentz γ factor. In this case $\chi \approx 2\gamma\xi\omega_0/m$, with the laser frequency ω_0 and the invariant laser parameter $\xi \equiv |e|E/(m\omega_0)$.

As the probability of emitting a photon in a so-called formation length is of the order of the fine structure constant α [43], and since one laser period contains about ξ formation lengths [11], the average number of photons emitted by an electron in a laser period is $N_{\rm ph} \sim \alpha\xi$, and the electron energy loss due to radiation yields $\Delta\varepsilon \sim \alpha\xi\chi\varepsilon$. Thus, the radiation-dominated regime (RDR) can be characterized by the parameter $R \equiv \alpha\xi\chi \gtrsim 1$ [3]. For available petawatt infrared lasers, $I \lesssim 3 \times 10^{22}$ W/cm^2 [42] ($\xi \lesssim 200$), the RDR is usually achievable only if $\chi \gtrsim 1$, i.e., in the quantum regime of interaction. A peculiar RDR has been identified in [21], when RR in the classical regime becomes prominent at $\xi \sim 100$, though in a rather narrow range of parameters near the (so-called) reflection condition $\xi \approx 2\gamma$. It was concluded in [32] that the RR effects in the classical regime are mostly detectable through measurements of electron-beam properties. Various modifications of the radiation spectrum in the quantum RDR of Compton scattering were put forward in [23,24]; however, these are not easily discernible in an experiment and require an accurate quantitative measurement. The role of stochastic effects in the quantum RDR was further studied. Those yield an increase of the electron energy and transverse spreading [44,45] as well as an increased output of high-energy photons [23,39].

The aim of this Letter is to identify signatures of RR for Compton radiation spectra in the quantum RDR, which are easily detectable in an experiment due to distinct qualitative characteristics. The parameters $R \gtrsim 1$ and $\chi \lesssim 1$ are employed to ensure that pair-production effects are negligible while quantum-recoil effects remain important. We investigate features of the angle-resolved spectra of Compton radiation when an ultrarelativistic electron beam counterpropagates with a strong focused ultrashort laser pulse of variable duration. In particular, with increasing laser-pulse duration the angular spread of the main photon-emission region (MPER) is shown to initially rise in a narrow range due to laser focusing and then continuously decrease because of quantum RR. This unique behavior does not exist in the classical RR regime. The spectral bandwidths of the radiation in the quantum and classical regimes both monotonically decrease when the laser-pulse duration is increased, but the former is larger, by orders of magnitude, due to much stronger RR effects. The qualitative behaviors mentioned are observed in a broad range of laser and electron parameters. The electron dynamics including RR is described by classical equations of motion [24], while the emitted radiation is calculated quantum mechanically [11]. The simple quasiclassical approach for the electron dynamics is justified as the electron's de Broglie wavelength is much smaller than the laser wavelength, and it allows us to explore the role of the laser-focusing effect in the quantum RDR.

Usually, high laser intensities are obtained by focusing a laser beam to a spot size of the order of the wavelength. When, additionally, the laser pulse is of the duration of only few cycles, then the well-known paraxial approximation [46–50] is not suitable for its description. In this case the small diffraction parameter $(k_0 w_0)^{-1}$ is of the same order of magnitude as the temporal parameter $(\omega_0\tau_0)^{-1}$, where k_0, w_0, and τ_0 are the wave vector, waist radius, and pulse duration of the laser beam, respectively; the approximate solution of Maxwell equations should treat both parameters on equal footing. We consider a circularly polarized focused ultrashort laser pulse propagating along the z direction. The field of the laser pulse is derived in the Supplemental Material [51], analogous to [52]. Note that the temporal envelope of the laser beam is not factorized in this solution.

We describe RR as the emission of multiple photons during the electron motion in a laser field when the electron dynamics is accordingly modified following the photon emissions. In superstrong laser fields $\xi \gg 1$, the coherence length of the photon emission is much smaller than the laser wavelength [11] and the photon-emission probability is determined by the local electron trajectory, and, consequently, by the local value of the parameter χ. The differential probability per unit phase interval is [11,25]:

$$\frac{dW_{fi}}{d\eta d\tilde{\omega}} = \frac{\left\{\alpha\tilde{\chi}m^2\left[\int_{\tilde{\omega}_r}^{\infty} K_{5/3}(x)dx + \tilde{\omega}\tilde{\omega}_r\tilde{\chi}^2 K_{2/3}(\omega_r)\right]\right\}}{[\sqrt{3}\pi(k_{0i}\cdot p_i)]}, \quad (1)$$

where $\eta = \omega_0 t - k_0 z$, $\tilde{\omega} = k_{0i}\cdot k_i/(\tilde{\chi}k_{0i}\cdot p_i)$ is the normalized emitted photon energy, $\tilde{\chi} = 3\chi/2$, k_{0i}, k_i, and p_i are the four-vectors of the driving laser photon, the emitted photon, and the electron, respectively, and $\tilde{\omega}_r = \tilde{\omega}/\rho_0$ with recoil parameter $\rho_0 = 1 - \tilde{\chi}\,\tilde{\omega}$ (in the classical limit $\rho_0 \approx 1$). The characteristic energy of the emitted photon is determined from the relation $\tilde{\omega}_r \sim 1$ and yields the cutoff frequency $\omega_c \sim \chi\varepsilon/(2/3+\chi)$. The rate of the electron radiation loss is $\mathcal{I} = \int d\tilde{\omega}(k_{0i}\cdot k_i)dW_{fi}/(d\eta d\tilde{\omega})$. Implementing the radiation losses due to quantum RR into the classical dynamics of the electron leads to the following equation of motion [25]:

$$\frac{dp^\alpha}{d\tau} = \frac{e}{m}F^{\alpha\beta}p_\beta - \frac{\mathcal{I}}{m}p^\alpha + \tau_c\frac{\mathcal{I}}{\mathcal{I}_c}F^{\alpha\beta}F_{\beta\gamma}p^\gamma, \quad (2)$$

where τ is the proper time, $\tau_c \equiv 2e^2/(3m)$, and $\mathcal{I}_c = 2\alpha\omega^2\xi^2$ is the classical radiation loss rate.

To study signatures of quantum RDR, we employ electrons with an initial energy of 500 MeV to interact with counterpropagating strong laser pulses of peak intensity $I \approx 7\times 10^{22}$ W/cm^2 ($\xi = 230$, $\chi \approx 0.6$, and $R \approx 1$) with various durations. We first study the radiation spectra of a single electron and then proceed with the case of an electron beam. The radiation spectra in laser pulses of $\tau_0 = T_0, 1.5T_0$, and $5T_0$, with the laser period T_0, are illustrated in Fig. 1. The photon-emission direction is determined by the polar angle θ with respect to the laser-propagation direction and the azimuthal angle φ with respect to the x-z polarization plane. The distribution within $155° \le \theta \le 180°$ is investigated, where the emission is mostly concentrated. The left column shows the angular distribution of the radiation energy, $d\varepsilon/d\Omega$, with the solid angle Ω. The polar angle spread for the MPER (roughly the yellow color part) is the largest for $\tau_0 = 1.5T_0$, increasing when changing $\tau_0 = T_0$ to

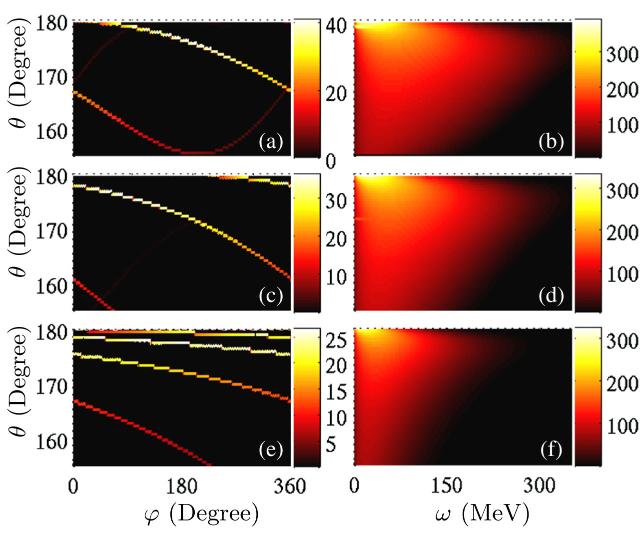

FIG. 1 (color online). The angle-resolved spectra of electron radiation in laser pulses of various durations: the left column displays $d\varepsilon/d\Omega$ [GeV/sr] and the right $d^2\varepsilon/d\omega d\Omega$ [1/sr] for (a)–(b) $\tau_0 = T_0$, (c)–(d) $\tau_0 = 1.5T_0$, and (e)–(f) $\tau_0 = 5T_0$. The laser wavelength is $\lambda_0 = 1$ μm while $w_0 = 10\lambda_0$, $\phi = 0$, $\xi = 230$, and $\gamma_0 = 1000$.

$\tau_0 = 1.5T_0$, and decreasing with further rising pulse duration. For each θ, there is a relevant $\varphi = \varphi_m$ where $d\varepsilon/d\Omega$ is maximal. The corresponding radiation spectrum, $d^2\varepsilon/(d\omega d\Omega)$ at $\varphi = \varphi_m$ is shown in the right column. While the value of φ_m depends on the laser carrier-envelope phase, the spectral intensity at this phase does not.

The dependences of both angular distribution and spectral bandwidth of the MPER on the laser-pulse duration are summarized in Fig. 2. The MPER is defined via the polar angular spread, $\Delta\theta = 180° - \theta_b$, with a boundary angle θ_b, where $d\varepsilon/d\Omega|_{\varphi=\varphi_m,\theta=\theta_b} = (d\varepsilon/d\Omega|_{\max})/2$. The corresponding spectral bandwidth $\Delta\omega$ of the radiation is defined as $\Delta\omega = \omega_b - \omega_{\min}$, with a boundary frequency ω_b, where $d^2\varepsilon/(d\omega d\Omega)|_{\theta=\theta_b,\omega=\omega_b} = (d^2\varepsilon/(d\omega d\Omega)|_{\theta=\theta_b,\max})/2$, and a minimal frequency $\omega_{\min} \approx 0$. As illustrated in Fig. 2(a), the boundary angle θ_b first decreases (i.e., $\Delta\theta$ increases) in an ultrashort pulse range $\tau_0 \lesssim 1.5T_0$, no matter whether RR effects are included, because of the laser-focusing effect (explained later). When the laser-pulse duration is further increased, the boundary angle θ_b monotonically rises (i.e., $\Delta\theta$ decreases) if the quantum RR effect is included (red dashed curve with square marks), and it almost remains unaltered if the RR effect is artificially removed in Eq. (2) (green dotted curve with diamond marks). In Fig. 2(b), the spectral bandwidth $\Delta\omega = \omega_b$ monotonically decreases with rising laser-pulse duration if quantum RR is taken into account, and it is almost constant when RR is neglected. Therefore, the signatures of RR in the emission spectra are easily distinguishable. Note that if the quantum effects (the quantum-recoil effect and the comparatively negligible radiation effect induced by electron spin) are artificially removed, while keeping RR fully classical, the variation dynamics within the MPER remains qualitatively similar but with apparent quantitative differences (cyan solid curves with circle marks).

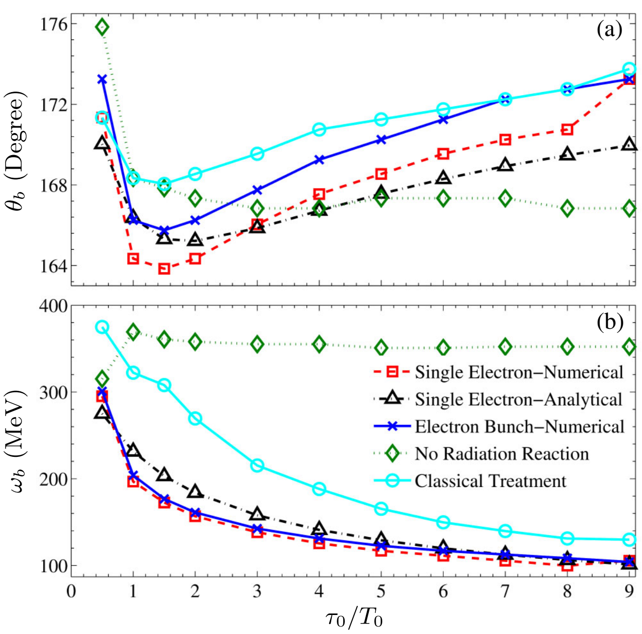

FIG. 2 (color online). The quantum RR signatures in the quantum RDR. The boundary angle θ_b (a) and the boundary frequency ω_b (b) of the emitted photons are displayed in dependence on the laser-pulse duration. The parameters employed are equal to those of Fig. 1.

Furthermore, our quantitative analysis shows that the discussed signatures of quantum RDR (when $R \gtrsim 1$ and $\chi \lesssim 1$) are clearly measurable in a broad range of parameters $\xi \lesssim \gamma \lesssim 20\xi$. In the extreme conditions $\gamma \gg \xi$ or $\gamma \ll \xi$, either the electron-deflection angle with respect to the laser propagation axis $\theta_e \sim \xi/\gamma$ is vanishing and the photon emission is mostly along a polar angle $\theta = 180°$, or the electron is quickly reflected by the laser pulse and emits within a very narrow angular spread near $\theta = 0°$. Thus, the signatures require $\xi \sim \gamma$; in this case the RDR regime $R \gtrsim 1$ is equivalent to the quantum regime $\chi \gtrsim 1$, while the classical RR regime $\chi \ll 1$ is tantamount to the out-of-RDR limit $R \ll 1$. Let us briefly discuss how the RR signatures considered here behave in a typical classical RR regime. We employ $\gamma = 100$ and $\xi = 100$ to obtain $\chi \approx 10^{-2}$ and $R \approx 10^{-2}$. As presented in Fig. 3, the behavior of the boundary angle θ_b vs the pulse duration is qualitatively different from that in the quantum RDR discussed above, since the RR effect is much smaller in the classical regime. While the boundary frequency ω_b monotonically reduces with the increase of the laser pulse, its magnitude is roughly two orders of magnitude lower than that in the quantum RDR.

To explain the properties of the MPER highlighted in Fig. 2, the corresponding electron dynamics is analyzed in Fig. 4. The maximal value of the parameter χ reduces with the increase of the pulse duration due to RR, as shown in Fig. 4(a). The radiation loss rate, $d\varepsilon/d\eta$, follows the behavior of the χ parameter as expected, cf. Figs. 4(a) and 4(b), which also can be analytically estimated as follows. The radiation loss in the coherence length $\Delta\eta_{\mathrm{coh}} \sim 2\pi/\xi$ can be estimated as $\Delta\varepsilon \sim \alpha\omega_c$, with the emission cutoff frequency $\omega_c \sim m\gamma\chi/(2/3+\chi)$, which yields the radiation loss rate $\mathcal{I} = d\varepsilon/d\eta \sim \Delta\varepsilon/\Delta\eta_{\mathrm{coh}} \sim \alpha\omega_c\xi/(2\pi) \propto \chi^2$, in line with the numerical result. The instantaneous momentum directions of the scattered electron are presented in Fig. 4(c), from which the photon-emission direction can be deduced, because an ultrarelativistic electron emits along the momentum

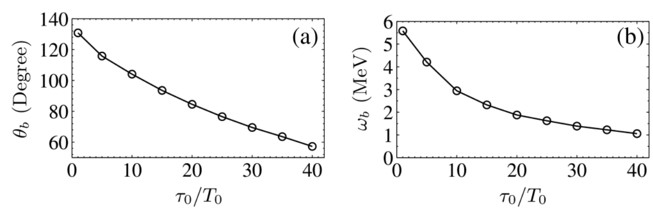

FIG. 3. The RR signatures in the classical RR regime. The variation of (a) the boundary angle θ_b and (b) the boundary frequency ω_b is displayed versus the laser-pulse duration. $\xi = 100, \gamma = 100$, and the other parameters are equal to those of Fig. 1.

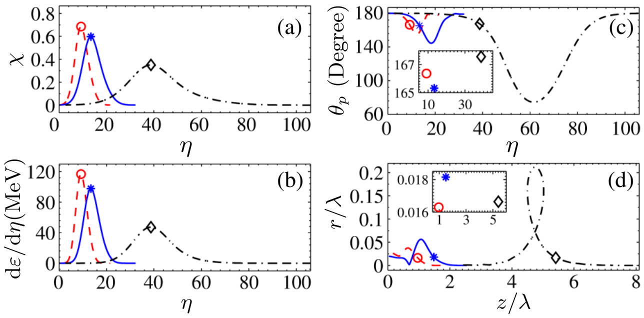

FIG. 4 (color online). The electron dynamics in counterpropagating laser pulses of various durations. The red dashed, blue solid, and black dash-dotted curves correspond to the laser-pulse durations $\tau_0 = T_0$, $\tau_0 = 1.5T_0$, and $\tau_0 = 5T_0$, respectively. Other parameters are equal to those of Fig. 1. The marks point out the places where the corresponding χ is maximal. The insets in (c) and (d) show the details of the main plot.

direction. For a longer laser pulse the angular distribution of photon emission is broader, but the MPER only concentrates in a narrow range near the $-z$ axis, where χ is very large. When the electron energy approaches the condition $\gamma \approx \xi/2$ due to radiation loss, the electron could be reflected by the laser pulse [see the loop in Fig. 4(d)]. Consequently, the backwards emission spectra can be observed even though its intensity is rather small compared with that in the MPER, and it also exists in the classical RR regime with a much narrower parameter range [21]. The insets in Figs. 4(c) and 4(d) clearly show that the polar angle corresponding to the χ maximum is largest for the case of $\tau_0 = 1.5T_0$, which is consistent with the θ_b behavior of the MPER. When the electron moves towards the laser-pulse center, the ξ parameter keeps increasing from zero to its peak, while the electron γ factor continuously reduces due to the radiation loss. Consequently, the parameter $\chi \propto \xi\gamma$ achieves the maximum at an intermediate laser phase η_m prior to the laser-pulse peak, and the electron transverse momentum at this moment is $p_{\perp m} \sim m\xi(\eta_m)$. In a longer laser pulse the electron energy decrease is larger and, consequently, the χ maximum is achieved during a longer travelled distance to the peak of the pulse; i.e., $\xi(\eta_m)$ and $p_{\perp m} \sim m\xi(\eta_m)$ are smaller, yielding a reduction of the emission angle $\theta \sim p_{\perp m}/p_{\parallel m}$. This can be seen by comparing the two cases of $\tau_0 = 1.5T_0$ and $\tau_0 = 5T_0$. However, in ultrashort pulses with duration $\tau_0 \lesssim 1.5T_0$, the variation gradient of the ξ parameter is more significant than that of γ due to the strong focusing effect, and the former is larger in a shorter laser pulse. Thus, the laser field at the χ maximum is larger for a shorter laser pulse. This is evident in comparing the emission boundary angle and the transverse distance at the χ maximum for $\tau_0 = T_0$ and $\tau_0 = 1.5T_0$ in Figs. 4(c) and 4(d). Moreover, the boundary angle θ_b and frequency ω_b can be analytically estimated via the polar angle of the electron momentum and the cutoff frequency ω_c, respectively, at the moment when the analytical radiation loss rate $d\varepsilon/d\eta$ is largest (i.e., χ is maximal), as shown in Fig. 2 (black dash-dotted curves with triangle marks), which qualitatively agree with the numerical results.

We proceed discussing the signatures of quantum RR in the case of an electron bunch. The following parameters are used: an electron bunch of cylindrical shape oriented along the z axis, with a bunch length $l_e = 6\ \mu$m and a bunch radius $w_e = 3\ \mu$m, containing $N_e = 10^7$ electrons. The angular spread of the bunch should be much smaller than $\Delta\theta \sim 10°$. The density of the bunch is $n_e = 5.9 \times 10^{16}$ cm^{-3}, and the relative loss of the laser energy due to Compton scattering for this number of electrons is estimated to be 10^{-6}, which justifies the external field approximation for the laser field. An electron beam of such density and an energy of 500 MeV is achievable via laser-plasma acceleration in an all-optical setup [53]. The space-charge force $F_C \sim 2\pi\alpha n_e w_e$ will be negligible with respect to the laser force $F_L \sim \xi m\omega_0$ in this case, as $F_C/F_L \sim 10^{-8}$. The dependences of θ_b and ω_b on the laser-pulse duration for the emission of the electron bunch (blue solid curves with cross marks) in Fig. 2 remain qualitatively unaltered compared with those of the single-electron case. The RR signatures under consideration persist when the laser waist radius w_0 and the electron-beam radius w_e are within the limits of $w_0 \gtrsim 4\lambda_0$ and $w_e \lesssim w_0/2$. Moreover, we estimate the number of laser shots to collect sufficient statistics for the observation of quantum RR signatures. For instance, the total probability of photon emission in the case of $\tau = 5T_0$ is $W_{\rm ph}^{\rm tot} \approx 39.42$, while the probability for the photon emission in $d\varepsilon/d\Omega|_{\max}$ and $d\varepsilon/d\Omega|_{\varphi=\varphi_m,\theta=\theta_b}$ yields $W_{\rm ph}^m \approx 0.0027$ and $W_{\rm ph}^b \approx 0.007$, respectively. The relative signal $|W_{\rm ph}^b - W_{\rm ph}^m|/W_{\rm ph}^{\rm tot} \approx 10^{-4}$ will be larger than the statistical error $\delta_s = (W_{\rm ph}^{\rm tot} N_e N_{\rm shot})^{-1/2} \sim 10^{-5}$ when the number of laser shots is $N_{\rm shot} = 10$. The probability of a photon decaying into an electron-positron pair for the maximal $\chi_{\rm photon} \approx 0.33$ is estimated to be 10^{-4} and negligible.

Concluding, we have identified signatures of quantum RDR in the dependence of both the angular spread and the spectral bandwidth of Compton radiation spectra on the laser-pulse duration, which are distinct from those in the classical RR regime. Because of an interplay between laser-beam focusing and quantum RR effects, the angular spread of the main photon-emission region has a prominent maximum at an intermediate pulse duration and decreases along the further increase of the pulse duration, and the spectral bandwidth monotonically decreases with rising pulse duration. These signatures are robust and observable in a broad range of electron and laser-beam parameters.

*Jian-Xing.Li@mpi-hd.mpg.de
†k.hatsagortsyan@mpi-hd.mpg.de
‡keitel@mpi-hd.mpg.de

[1] K. T. Phuoc, S. Corde, C. Thaury, V. Malka, A. Tafzi, J. P. Goddet, R. C. Shah, and S. S. A. Rousse, Nat. Photonics **6**, 308 (2012).

[2] S. Corde, K. Ta Phuoc, G. Lambert, R. Fitour, V. Malka, A. Rousse, A. Beck, and E. Lefebvre, Rev. Mod. Phys. **85**, 1 (2013).
[3] A. Di Piazza, C. Müller, K. Z. Hatsagortsyan, and C. H. Keitel, Rev. Mod. Phys. **84**, 1177 (2012).
[4] K. Achterhold, M. Bech, S. Schleede, G. Potdevin, R. Ruth, R. Loewen, and F. Pfeiffer, Sci. Rep. **3**, 1313 (2013).
[5] The Extreme Light Infrastructure (ELI), http://www.eli-laser.eu/.
[6] S. Chen, N. D. Powers, I. Ghebregziabher, C. M. Maharjan, C. Liu, G. Golovin, S. Banerjee, J. Zhang, N. Cunningham, A. Moorti, S. Clarke, S. Pozzi, and D. P. Umstadter, Phys. Rev. Lett. **110**, 155003 (2013).
[7] N. D. Powers, I. Ghebregziabher, G. Golovin, C. Liu, S. Chen, S. Banerjee, J. Zhang, and D. P. Umstadter, Nat. Photonics **8**, 28 (2014).
[8] I. I. Goldman, Zh. Eksp. Teor. Fiz. **46**, 1412 (1964) [Sov. Phys. JETP **19**, 954 (1964)].
[9] A. I. Nikishov and V. I. Ritus, Zh. Eksp. Teor. Fiz. **46**, 776 (1964) [Sov. Phys. JETP **19**, 529 (1964)].
[10] L. S. Brown and T. W. Kibble, Phys. Rev. **133**, A705 (1964).
[11] V. I. Ritus, J. Sov. Laser Res. **6**, 497 (1985).
[12] J. Koga, T Zh. Esirkepov, and S. V. Bulanov, Phys. Plasmas **12**, 093106 (2005).
[13] M. Abraham, *Theorie der Elektrizität* (Teubner, Leipzig, 1905).
[14] H. A. Lorentz, *The Theory of Electrons* (Teubner, Leipzig, 1909).
[15] P. A. M. Dirac, Proc. R. Soc. A **167**, 148 (1938).
[16] L. D. Landau and E. M. Lifshitz, *The Classical Theory of Fields* (Elsevier, Oxford, 1975).
[17] W. Heitler, Math. Proc. Cambridge Philos. Soc. **37**, 291 (1941).
[18] A. H. Wilson, Math. Proc. Cambridge Philos. Soc. **37**, 301 (1941).
[19] W. Heitler, *The Quantum Theory of Radiation* (Dover Publications, New York, 1984).
[20] J. M. Jauch and F. Rohrlich, *The Theory of Photons and Electrons* (Springer-Verlag, Berlin, 1976).
[21] A. Di Piazza, K. Z. Hatsagortsyan, and C. H. Keitel, Phys. Rev. Lett. **102**, 254802 (2009).
[22] I. V. Sokolov, N. M. Naumova, J. A. Nees, G. A. Mourou, and V. P. Yanovsky, Phys. Plasmas **16**, 093115 (2009).
[23] A. Di Piazza, K. Z. Hatsagortsyan, and C. H. Keitel, Phys. Rev. Lett. **105**, 220403 (2010).
[24] I. V. Sokolov, N. M. Naumova, J. A. Nees, and G. A. Mourou, Phys. Rev. Lett. **105**, 195005 (2010).
[25] I. V. Sokolov, J. A. Nees, V. P. Yanovsky, N. M. Naumova, and G. A. Mourou, Phys. Rev. E **81**, 036412 (2010).
[26] I. V. Sokolov, N. M. Naumova, and J. A. Nees, Phys. Plasmas **18**, 093109 (2011).
[27] S. V. Bulanov, T. Z. Esirkepov, M. Kando, J. K. Koga, and S. S. Bulanov, Phys. Rev. E **84**, 056605 (2011).
[28] C. Harvey, T. Heinzl, and M. Marklund, Phys. Rev. D **84**, 116005 (2011).
[29] T. Nakamura, J. K. Koga, T. Z. Esirkepov, M. Kando, G. Korn, and S. V. Bulanov, Phys. Rev. Lett. **108**, 195001 (2012).
[30] M. Tamburini, T. V. Liseykina, F. Pegoraro, and A. Macchi, Phys. Rev. E **85**, 016407 (2012).
[31] C. Harvey and M. Marklund, Phys. Rev. A **85**, 013412 (2012).
[32] A. G. R. Thomas, C. P. Ridgers, S. S. Bulanov, B. J. Griffin, and S. P. D. Mangles, Phys. Rev. X **2**, 041004 (2012).
[33] T. Schlegel and V. T. Tikhonchuk, New J. Phys. **14**, 073034 (2012).
[34] R. R. Pandit and Y. Sentoku, Phys. Plasmas **19**, 073304 (2012).
[35] F. Mackenroth and A. Di Piazza, Phys. Rev. Lett. **110**, 070402 (2013).
[36] R. Capdessus, E. d'Humières, and V. T. Tikhonchuk, Phys. Rev. Lett. **110**, 215003 (2013).
[37] N. Kumar, K. Z. Hatsagortsyan, and C. H. Keitel, Phys. Rev. Lett. **111**, 105001 (2013).
[38] M. Tamburini, C. H. Keitel, and A. Di Piazza, Phys. Rev. E **89**, 021201 (2014).
[39] T. G. Blackburn, C. P. Ridgers, J. G. Kirk, and A. R. Bell, Phys. Rev. Lett. **112**, 015001 (2014).
[40] H. R. Reiss, J. Math. Phys. (N.Y.) **3**, 59 (1962).
[41] J. Schwinger, Phys. Rev. **82**, 664 (1951).
[42] V. Yanovsky, V. Chvykov, G. Kalinchenko, P. Rousseau, T. Planchon, T. Matsuoka, A. Maksimchuk, J. Nees, G. Cheriaux, G. Mourou, and K. Krushelnick, Opt. Express **16**, 2109 (2008).
[43] I. I. Abbasov, B. M. Bolotovskii, and V. A. Davydov, Usp. Fiz. Nauk **149**, 709 (1986) [Sov. Phys. Usp. **29**, 788 (1986)].
[44] N. Neitz and A. Di Piazza, Phys. Rev. Lett. **111**, 054802 (2013).
[45] D. G. Green and C. N. Harvey, Phys. Rev. Lett. **112**, 164801 (2014).
[46] Y. I. Salamin, S. Hu, K. Z. Hatsagortsyan, and C. H. Keitel, Phys. Rep. **427**, 41 (2006).
[47] Y. I. Salamin and C. H. Keitel, Phys. Rev. Lett. **88**, 095005 (2002).
[48] Y. I. Salamin, Appl. Phys. B **86**, 319 (2007).
[49] J. Li, W. Zang, and J. Tian, Opt. Express **17**, 4959 (2009).
[50] J.-X. Li, W.-P. Zang, Y.-D. Li, and J.-G. Tian, Opt. Express **17**, 11850 (2009).
[51] See Supplemental Material at http://link.aps.org/supplemental/10.1103/PhysRevLett.113.044801, which includes Refs. [47,52,54].
[52] E. Esarey, P. Sprangle, M. Pilloff, and J. Krall, J. Opt. Soc. Am. B **12**, 1695 (1995).
[53] E. Esarey, C. B. Schroeder, and W. P. Leemans, Rev. Mod. Phys. **81**, 1229 (2009).
[54] Q. Lin, J. Zheng, and W. Becker, Phys. Rev. Lett. **97**, 253902 (2006).